



## Effect of Allophane from Gamalama Volcanic Soil on Properties of BiOI-Allophane Composite

INDRA CIPTA<sup>1,\*</sup>, NUR A. LIMATAHU<sup>1</sup>, N.A. ST. HAYATUN<sup>1</sup>, INDRIANA KARTINI<sup>2</sup> and YATEMAN ARRYANTO<sup>2</sup>

<sup>1</sup>Department of Chemistry Education, Faculty of Teacher Training and Education, Khairun University, Ternate, Indonesia

<sup>2</sup>Department of Chemistry, Faculty of Mathematics and Natural Science, Universitas Gadjah Mada, Yogyakarta, Indonesia

\*Corresponding author: E-mail: [indra.chemy@gmail.com](mailto:indra.chemy@gmail.com)

Received: 9 November 2016;

Accepted: 13 January 2017;

Published online: 10 March 2017;

AJC-18296

Effect of allophane from Gamalama volcanic soil to the properties of BiOI-allophane had been studied in this work. Composite of BiOI-allophane from Gamalama volcanic soil has the potential to be applied as a photocatalyst or photofuel under visible light radiation. Increasing the amount of allophane increase the surface area of 30.122 to 63.240 m<sup>2</sup> g<sup>-1</sup>. E<sub>g</sub> value of the resulted composite vary from 1.6-2.4 eV due to the various allophane amount.

**Keywords:** Allophane, Composite, BiOI, Visible light, Surface area.

### INTRODUCTION

Semiconductor material could potentially be used as an electrode photofuel cells to generate electricity or as a photocatalyst decomposing contaminants [1-3]. Among some semiconductor materials, TiO<sub>2</sub> has a high photocatalytic activity and high stability. But performance is limited to the UV region caused by the large energy gap. UV rays that enter the earth's surface are so few that the application would be very limited in both TiO<sub>2</sub> as a photocatalyst or photofuel. It's required a semiconductor material that can absorb visible light waves. BiOI is a semiconductor material with a band gap (E<sub>g</sub>) value between 1.83-1.7 eV and able to absorb visible light ( $\lambda < 700$  nm) [3]. Various synthesis methods of BiOI have been studied and ability as photocatalysts under visible light has already been studied.

Semiconductor materials performance as photocatalysts and photofuel depends on sorption capacity and the band gap energy. Sorption capacity of a material depends heavily on surface area and particle size. To increase the adsorption capacity, various methods have been tried and known in advance. One method that is most often attempted, by composites the semiconductor material with a porous material, such as zeolite, clay minerals, silica and activated carbon [4]. Composite of semiconductor materials such as TiO<sub>2</sub> montmorillonite [5], kaolinite and hectorit [6] and hydroxyapatite [7], had been proven able to improve the photocatalytic activity and affected the value of band gap energy (E<sub>g</sub>). Allophane from the volcanic soil of mount gamalama was chosen as a host material BiOI nanocomposite. Allophane is expected to increase the surface

area of BiOI. This study was used a hydrothermal method to distribute BiOI into allophane framework. The influence of the allophane through the BiOI-allophane composites are discuss in this work.

### EXPERIMENTAL

Allophane put into the mix of 5 mmol Bi(NO<sub>3</sub>)<sub>3</sub>·5H<sub>2</sub>O and 5 mmol KI previously dissolved separately by using 15 mL of ethylene glycol and 15 mL of deionized water. Composites were made using 0.25 g allophane (BiO-A1), 0.5 g (BiO-A2) and 1 g (BiO-A3). The mixture is then stirred for 30 min and then put in autoclave for hydrothermal treatment in 180 °C for 24 h. The resulting precipitates were collected by centrifugation, washed with deionized water to remove unreacted ions. The composites were then dried at 80 °C for 8 h and characterized by using FTIR, XRD, SEM, TEM and BET analysis, as well as UV visible diffuse reflectance to determine the effect of the amount of allophane.

### RESULTS AND DISCUSSION

XRD characterization results of allophane, BiOI, Bi-A1, Bi-A2 and Bi-A3 is shown in Fig. 1. Based on the picture, it appears that there are some differences between the diffraction peaks between the raw material and the composite. Allophane showed low diffraction peaks in each diffraction angle as characteristic for amorphous materials. BiOI diffraction peaks are not much different from that indicated by BiO-A1, BiO-A2 and BiO-A3. Diffraction peaks of BiOI at 25°, 29° and 31° shown increases of intensity that may be caused by changes

in particle size BiOI which becomes smaller with the presence of allo-phane. In addition, it can be seen several peaks become wider that may be caused by the presence of amorphous material allophane that affect the size of the crystal unit BiOI [8].

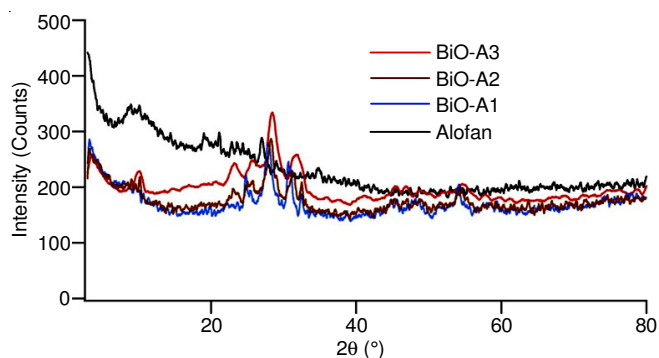


Fig. 1. XRD diffractograms of allophane, BiO-A1, BiO-A2, BiO-A3

Distribution of BiOI on the surface allophane more evenly due to the increasing amount of allophane. It is shown in Fig. 2, SEM images of the allophane, BiO-A1, BiO-A2 and BiO-A3.

SEM image of BIO-A1, showed that there are many BiOI still present in plate form. It is different from the composite BiO-A2 and BiO-A3 where BiOI dispersed with form “like a net” covered the surface of allophane. Diameter composite BiO-A2 and BiO-A3 are not homogeneous due to the nature of allophane, irregular spherule with varying diameter [9-11]. Increasing the amount of allophane cause BiOI-Allophane diameter size be-comes smaller. Fig. 2 shows the BiO-A2 size diameter between 1-2.5  $\mu\text{m}$ , BiO-A3 between 0.25-1.5  $\mu\text{m}$ .

The surface area measurement of allophane, BiOI, BiO-A1, BiO-A2 and BiO-A3 (Table-1) shows that the surface area increases after BiOI be composited with the allophane which has a surface area of 125-158  $\text{m}^2 \text{g}^{-1}$ . Increased of surface area is also shown on the composite sample BiO-A1, BiO-A2, BiO-A3 ranging from 30.796, 38.966 and 63.240  $\text{m}^2 \text{g}^{-1}$ , respectively.

BiOI surface area showed changes after its composite with allophane. Distribution of BiOI in the framework of allophane cause BiOI particle size becomes smaller so that the surface area to be increased. BET analysis results from each of the resultant composite indicates excellent potential to be applied as a photocatalyst or photofuel. The resulting composite surface area is much larger than BiOI nanoplate and nanosheets

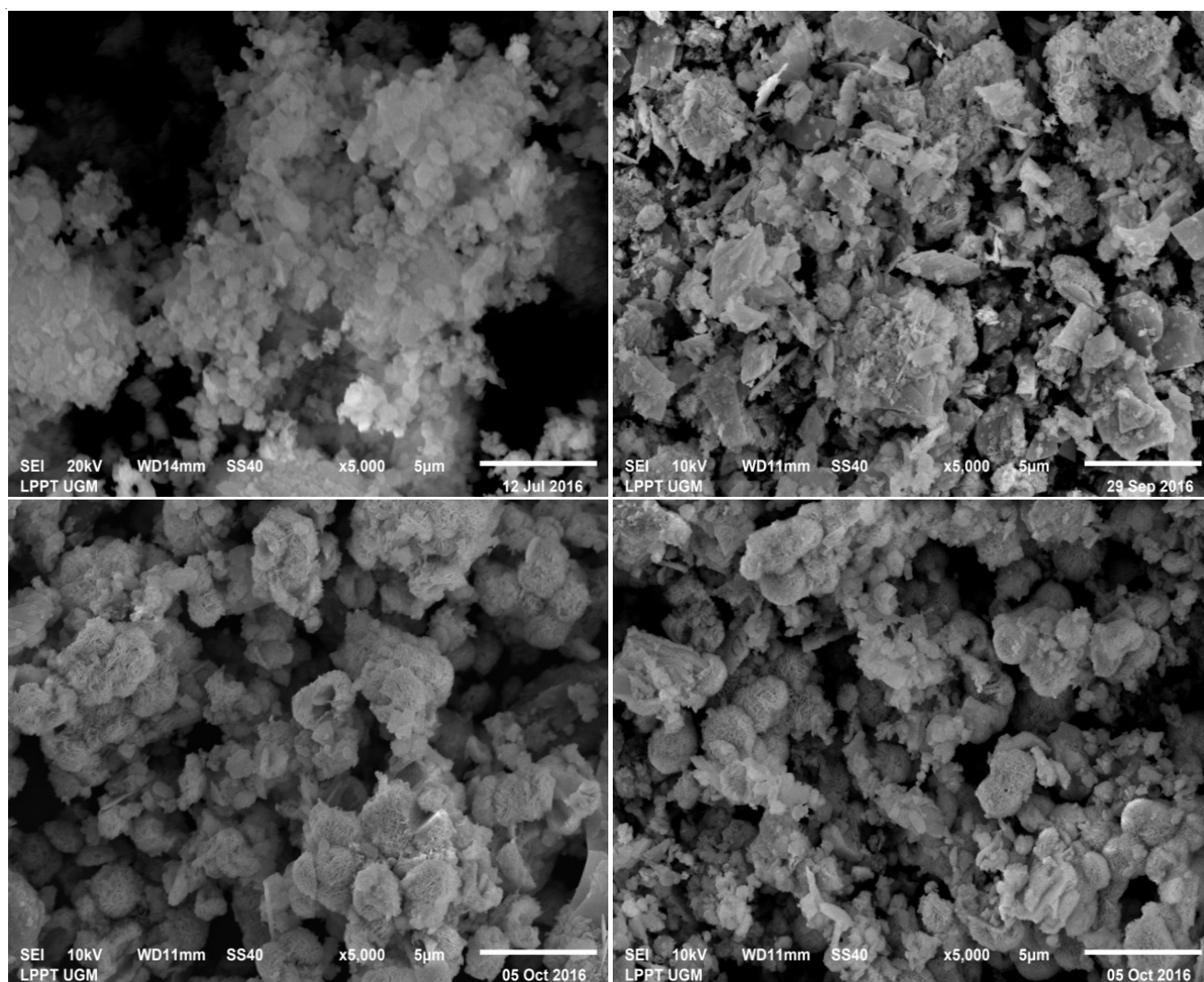


Fig. 2. SEM Images of (A) allophane; (B) BiO-A1; (C) BiO-A2; (D) BiO-A3

TABLE-1  
BET SURFACE ANALYZER,  $E_g$ ,  $E_{VB}$ ,  $E_{CB}$  DATA

Samples	$A_{BET}$ ( $m^2 g^{-1}$ )	$E_g$ (eV)	$E_{VB}$ (eV)	$E_{CB}$ (eV)
Allophane	125.158	—	—	—
BiOI	30.122	1.60	2.25	0.65
BiO-A1	30.796	1.75	2.32	0.57
BiO-A2	38.966	1.89	2.39	0.50
BiO-A3	63.240	2.40	2.65	0.25

produced by Lee *et al.* [12] and Li *et al.* [13] is 0.08-7.20  $m^2 g^{-1}$ , 22.3  $m^2 g^{-1}$ , respectively.

$$E_{VB} = \chi - E_e + 0.5 E_g \quad (1)$$

$$E_{CB} = E_{VB} - E_g \quad (2)$$

By using the UV spectral data-DRS band gap energy BiOI and the composites were determined using the Kubelka-Munk method. Valence band-edge potential ( $E_{VB}$ ) and the conduction band edge ( $E_{CB}$ ) is determined by using eqns. 1 and 2, where  $E_{VB}$  is valence band-edge potential ( $\chi$ ) are the electronegativity absolute constituent atoms,  $E_e$  energy of free electrons in the hydrogen scale (4.5 eV),  $E_g$  and the  $E_{CB}$  are respectively the energy band gap and the conduction band edge energy. The values of  $E_g$ ,  $E_{VB}$  and the  $E_{CB}$  are presented in Table-1. The  $E_g$  value of the sample BiOI, BiO-A1, BiO-A2 and BiO-A3 as shown in Table-1, respectively 1.60, 1.75, 1.89 and 2.4 eV. Extra allophane show the effect on the value of the energy band gap composites. Increasing the number of allophane used in composites caused greater value of  $E_g$ . The energy band gap of a semiconductor material that is between the valence band and the conduction band increases with decrease of particle size [14]. Bismuth oxyiodides has the ability to absorb visible light [8,15]. Samples BiOI, BiO-A1, BiO-A2 and BiO-A3 which resulted in this study are also demonstrated an ability to absorb visible light in the wavelength range 200-800 nm. This is verified by the results of the characterization of UV-visible diffuse reflectance (DRS) (Fig. 3). Based on the data presented in Table-1 and the spectra in Fig. 3 can be concluded that the composite BiOI-allophane from gamalama volcanic soil has the potential to be applied as electrodes fotofuel or photocatalyst with visible light irradiation. The composite's properties are affected by the amount of allophane.

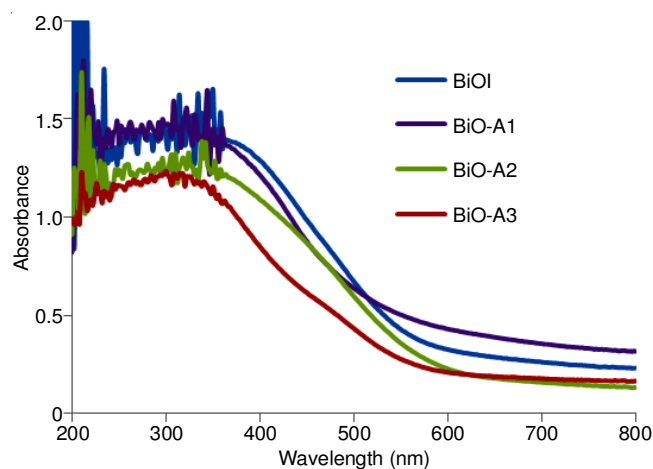


Fig. 3. UV-DRS spectra of BiOI and BiOI-Allophane composite

## Conclusion

Composite BiOI-allophane from gamalama volcanic soil has the potential to be applied as a photocatalyst or photofuel under visible light radiation. Increasing the amount of allophane increase the surface area of 30.122 to 63.240  $m^2 g^{-1}$ .  $E_g$  value of the resulted composite is vary from 1.6-2.4 eV due to the various amount of allophane.

## ACKNOWLEDGEMENTS

The authors thank the Ministry of Research Technology and Higher Education for funding this research through grants INSINAS 2016.

## REFERENCES

1. S. Min, F. Wang, Z. Jin and J. Xu, *Superlattices Microstruct.*, **74**, 294 (2014); <https://doi.org/10.1016/j.spmi.2014.07.003>.
2. H. Nisihikiori, K. Isomura, Y. Uesugi and T. Fujii, *Appl. Catal. B*, **106**, 250 (2011); <https://doi.org/10.1016/j.apcatb.2011.05.035>.
3. B. Wang, H. Zhang, X.-Y. Lu, J. Xuan and M.K.H. Leung, *Chem. Eng. J.*, **253**, 174 (2014); <https://doi.org/10.1016/j.cej.2014.05.041>.
4. M. Hojamberdiev, K. Katsumata, N. Matsushita and K. Okada, *Appl. Clay Sci.*, **101**, 38 (2014); <https://doi.org/10.1016/j.clay.2014.07.007>.
5. Y. Kameshima, Y. Tamura, A. Nakajima and K. Okada, *Appl. Clay Sci.*, **45**, 20 (2009); <https://doi.org/10.1016/j.clay.2009.03.005>.
6. D. Kibanova, M. Trejo, H. Destailats and J. Cervini-Silva, *Appl. Clay Sci.*, **42**, 563 (2009); <https://doi.org/10.1016/j.clay.2008.03.009>.
7. Y. Ono, T. Rachi, M. Yokouchi, Y. Kamimoto, A. Nakajima and K. Okada, *Mater. Res. Bull.*, **48**, 2272 (2013); <https://doi.org/10.1016/j.materresbull.2013.02.067>.
8. C. Liao, Z. Ma, X. Chen, X. He and J. Qiu, *Appl. Surf. Sci.*, **387**, 1247 (2016); <https://doi.org/10.1016/j.apsusc.2016.06.140>.
9. M.C. Floody, B.K.G. Theng and M.L. Mora, *Clay Miner.*, **44**, 161 (2009); <https://doi.org/10.1180/claymin.2009.044.2.161>.
10. B. Creton, D. Bougeard, K.S. Smirnov, J. Guilment and O. Poncelet, *J. Phys. Chem. C*, **112**, 358 (2008); <https://doi.org/10.1021/jp0738412>.
11. E.G. Garrido-Ramirez, B.K.G. Theng and M.L. Mora, *Appl. Clay Sci.*, **47**, 182 (2010); <https://doi.org/10.1016/j.clay.2009.11.044>.
12. W.W. Lee, C.-S. Lu, C.-W. Chuang, Y.-J. Chen, J.-F. Fu, C.-W. Siao and C.-C. Chen, *RSC Adv.*, **5**, 23450 (2015); <https://doi.org/10.1039/C4RA15072D>.
13. Y. Li, J. Wang, H. Yao, L. Dang and Z. Li, *J. Mol. Catal. A*, **334**, 116 (2011); <https://doi.org/10.1016/j.molcata.2010.11.005>.
14. A. Pourahmad and Sh. Sohrabnezhad, *Int. J. Nanosci. Nanotechnol.*, **5**, 35 (2009).
15. F. Chen, C. Niu, Q. Yang, X. Li and G. Zeng, *Ceram. Int.*, **42**, 2515 (2016); <https://doi.org/10.1016/j.ceramint.2015.10.053>.